KERNFORSCHUNGSZENTRUM

KARLSRUHE

August 1976 KFK 2337

Institut für Angewandte Kernphysik
Projekt Schneller Brüter

The Total Neutron Cross Section of ^{58}Fe in the Energy Range 7 to 325 keV

H. Beer, Li Dy Hong, F. Käppeler

GESELLSCHAFT
FÜR
KERNFORSCHUNG M.B.H.

KARLSRUHE

Als Manuskript vervielfältigt

Für diesen Bericht behalten wir uns alle Rechte vor

GESELLSCHAFT FÜR KERNFORSCHUNG M. B. H.

KARLSRUHE

KERNFORSCHUNGSZENTRUM KARLSRUHE

KFK 2337

Institut für Angewandte Kernphysik
Projekt Schneller Brüter

The Total Neutron Cross Section of ^{58}Fe in the Energy Range 7 to 325 keV

H. Beer, Li Dy Hong[+], F. Käppeler

[+] University of Heidelberg

Gesellschaft für Kernforschung mbH, Karlsruhe

ABSTRACT

The total neutron cross section of ^{58}Fe has been determined in the energy range 7-325 keV by a transmission measurement using enriched ^{58}Fe samples. The data have been shape fitted by means of an R-matrix multi-level formalism to extract resonance parameters for s- and $\ell > 0$ wave resonances. The s-wave strength function was determined to $S_o = (4.3 \pm 1.9) \times 10^{-4}$.

Der totale Neutronenquerschnitt von ^{58}Fe im Energiebereich 7-325 keV

ZUSAMMENFASSUNG

Der totale Neutronenquerschnitt von ^{58}Fe im Energiebereich 7-325 keV wurde durch eine Transmissionsmessung unter Verwendung angereicherter ^{58}Fe Proben bestimmt. Die Daten wurden durch Formanalyse mit dem R-Matrix-Formalismus ausgewertet, um Resonanzparameter für s- und $\ell > 0$ Wellen-Resonanzen abzuleiten. Die s-Wellen Stärkefunktion wurde zu $S_o = (4.3 \pm 1.9) \times 10^{-4}$ bestimmt.

INTRODUCTION

As part of a continuing effort to determine total and capture cross sections of medium weight nuclei the total neutron cross section of ^{58}Fe has been measured in the energy range 7-325 keV. Although ^{58}Fe has only 0.31 % natural abundance its resonance structure, if located in the resonance minima of ^{56}Fe, might contribute significantly to the total cross section of iron in structural materials of fast reactors. In addition, ^{59}Fe with a half life of 44 days is activated by neutron capture in ^{58}Fe.

The ^{58}Fe nucleus has not yet been studied experimentally. Information about its neutron strength is of interst for the investigation of the 3s giant resonance mass region at A $\sim$ 55.

From the view-point of astrophysics the neutron rich nuclide ^{58}Fe is of particular importance. To reproduce its stellar abundance neutron cross sections which allow an estimation of the influence of s-process formation are needed /1,2/. In the present work the observed resonance structure in the total cross section has been analysed by an R-matrix multilevel formalism and the resonance parameters for neutron scattering were extracted. From the resonance neutron widths and spacings the s-wave strength function was derived and compared with results of neighbouring nuclei.

EXPERIMENT

The measurement was carried out at the Karlsruhe 3 MV pulsed Van-de-Graaff accelerator using the time-of-flight technique. Neutrons were generated via the ^{7}Li (p,n)^{7}Be reaction in a Li-target with protons of 1 ns pulse widths and a repetition rate of 250 kHz.

In Fig. 1 a scheme of the experimental set-up is displayed. At a flight path of 499.1 cm a Li-loaded glass scintillator[+] (4 3/8" dia x 1/2" thickness, 6.6 % Li enriched in ^{6}Li to 95 %) was installed for neutron detection.

[+] NE 905 Nuclear Enterprise

The Li-glass was coupled to an XP-1040 photomultiplier (Fig. 2). Two samples and an empty sample container were cycled successively into the collimated neutron beam. The cycle period was controlled by a proton beam current integrator. The samples consisted of powdered oxide (Fe_2O_3) pressed into thin walled Al-containers of 1.1 cm diameter. The sample characteristics (amounts and enrichments) are given in Table 1.

The electronical arrangement of the experiment is shown in Fig. 3. For the derivation of a time signal the anode signals of the XP-1040 photomultiplier were clipped and discriminated against signal noise. The pulse height information of the detected neutrons was taken from the 10th dynode. After amplification the signals were passed through a single channel analyser (SCA). In Fig. 4 a typical neutron distribution measured with the Li-glass detector is seen. The start signal for the time-to-amplitude converter (TAC) was obtained via a coincidence required between time signal and pulse height signal. The stop signal was delivered from the Van-de-Graaff proton pick-up. Time-of-flight spectra with and without the samples were recorded separately into 2048 channel arrays by a 510 CAE on-line computer.

DATA ANALYSIS

The transmission was computed from time-of-flight spectra with and without sample. Backgrounds were determined from the region between γ-flash and onset of the fastest neutrons. The transmission data were shape fitted by means of the Fortran IV code Fanal II /3/, which uses an R-matrix formalism as described by Lane and Thomas /4/. The program delivers chi-square fits to the experimental data in an iterative way starting from a preselected set of resonance parameters which are improved in the procedure of each iteration. The computations are terminated when the relative change between two iterations attains a prescribed limit. The computer analysis included all the contaminant iron isotopes and the oxygen content of the sample. The oxygen cross section was generated using a potential scattering radius of 5.6 fm. This choice delivered slightly

energy dependent cross section values in the studied energy range in accordance with the data of Mooring et al. /5/. For the ^{54}Fe and ^{57}Fe impurites resonance parameters determined by Beer and Spencer /6/ and Rohr and Müller /7/ were used. The sizeable ^{56}Fe content was taken into account by selected resonance parameters which are mainly those of Pandey et al. /8/.

The final best fits of the transmission data with thin and thick sample together with the resolution broadened cross section of the pure ^{58}Fe isotope generated from the extracted resonance parameters are shown in Figures 5 to 8. The resonance parameters are listed in Table 2. In addition to the resonance energies and widths the potential scattering radius and a strength function like variable S_J' which describes the influence of distant resonances are given.

DISCUSSION

The transmission data show the influence of the sizeable ^{56}Fe impurity present in the sample material. Energy regions where large scattering resonances of ^{56}Fe are visible have been indicated by arrows in Figures 5 to 8. In the measured energy interval 7-325 keV 10 s-wave resonances and 8 $\ell > 0$ wave resonances have been observed in ^{58}Fe. So far no ^{58}Fe data have been reported in the investigated energy range which can be compared with the present results.

The resonance parameters for s-wave resonances were used to calculate the average resonance spacing and the s-wave strength function S_o. S_o is defined in the following way:

$$S_o = \sum_{i=1}^{N} \Gamma^o_{ni} \; / \; \Delta E \qquad (1)$$

where Γ^o_{ni} is the i-th reduced neutron width of a total of N analysed s-wave resonances in the energy interval ΔE. For the energy range 7-325 keV a spacing $\bar{D}$ = 31.8 keV and an ^{58}Fe strength function $S_o = (4.3 \times 1.9) \times 10^{-4}$ was derived.

^{58}Fe is close to the maximum of the 3s giant resonance at about mass A ≃ 55. Although this nucleus exhibits not the exceptional strength found in ^{54}Fe /6/, its strength function is much higher than that of ^{56}Fe and shows about the same magnitude as ^{57}Fe. The strength functions of the isotones ^{59}Co and ^{60}Ni are somewhat smaller than the ^{58}Fe result (Table 3).

The relatively high strength function of ^{58}Fe in spite of its low neutron binding energy reflects the influence of the large scattering resonances observed.

ACKNOWLEDGEMENT

The authors would like to express their appreciation for the separated ^{58}Fe isotope which was made available through the USAEC-EANDC loan pool. We are indebted to G. Rupp for his help in setting up the experiment. The diligence of the Van-de-Graaff crew in maintaining the required beam conditions is appreciated.

REFERENCES

/1/ J.G. Peters, W.A. Fowler, D.D. Clayton, J. Astrophys. 173, (1972) 637.

/2/ H.D. Zeh, Astronom. & Astrophys. 28 (1973) 427.

/3/ F.H. Fröhner, KFK-2129 (1976).

/4/ A.M. Lane, R.G. Thomas, Rev. Mod. Phys. 30 (1958) 257.

/5/ F.P. Mooring, J.E. Monahan, C.M. Huddleston, Nucl. Phys. 82 (1966) 16.

/6/ H. Beer, R.R. Spencer, Nucl. Phys. A 240 (1975) 29.

/7/ G. Rohr, K.-N. Müller, Z. Physik 227 (1969) 1.

/8/ M.S. Pandey, J.B. Garg, J.A. Harvey, W.M. Good, Proc. Conf. Nucl. Cross Section and Technology, Washington 1975, Vol. II, p. 748.

/9/ K.K. Seth, Nucl. Data A2 (1966) 299.

/10/ R.G. Stieglitz, R.W. Hockenbury, R. C. Block, Nucl. Phys. A 163 (1971) 592.

Table 1

Sample Characteristics

Sample Material[+]		Isotopic Composition Atomic Percent			
g Fe_2O_3	atoms/barn	^{54}Fe	^{56}Fe	^{57}Fe	^{58}Fe
2.4157	0.03959	1.44	30.78	2.68	65.09
7.1509	0.11720				

[+] Samples were obtained through the USAEC-EANDC loan pool

Table 2

The Resonance Parameters of ^{58}Fe

E_o (keV)	ℓ	$g\Gamma_n$ (keV)
10.339 ± 0.047	0	0.416 ± 0.005
19.346 ± 0.095	>0	∿0.0026
26.10 ± 0.13	>0	∿0.0068
34.67 ± 0.19	>0	∿0.0079
37.66 ± 0.21	>0	0.027 ± 0.008
43.55 ± 0.25	0	6.37 ± 0.21
54.72 ± 0.33	>0	0.057 ± 0.010
62.04 ± 0.39	>0	0.053 ± 0.014
67.18 ± 0.44	0	0.997 ± 0.049
93.90 ± 0.69	0	12.23 ± 0.78
121.67 ± 0.97	0	2.67 ± 0.21
131.3 ± 1.1	>0	0.200 ± 0.022
152.7 ± 1.4	>0	0.285 ± 0.031
179.5 ± 1.7	0	2.39 ± 0.25
241.2 ± 2.6	0	10.8 ± 1.4
266.0 ± 2.9	0	9.2 ± 1.3
309.9 ± 3.7	0	3.10 ± 0.47
321.0 ± 3.9	0	1.03 ± 0.16

$a_J = 5.6$ fm $\qquad S_J^1 = 2.5 \times 10^{-4}$

Table 3

s-Wave Strength Functions of Nuclei in the Vicinity of ^{58}Fe

Target Nucleus	Neutron Binding Energy (MeV)	Strenght Function $S_o \times 10^{-4}$
^{54}Fe	9.299	7.8 ± 3.4 [a]
^{56}Fe	7.641	1.6 ± 0.5 [b]
^{57}Fe	10.042	4.5 ± 1.1 [c]
^{58}Fe	6.585	4.3 ± 1.9
^{59}Co	7.490	3.8 ± 1.6 [b]
^{60}Ni	7.821	2.95 ± 1.04 [d]

a) Ref. /6/

b) Ref. /9/

c) Ref. /7/

d) Ref. /10/

FIGURE CAPTIONS

Fig. 1: Scheme of the experimental set-up

Fig. 2: Sketch of the Li-glass detector.

Fig. 3: Block diagram of the electronic arrangement.

Fig. 4: Neutron pulse height distribution measured with the Li-glass detector.

Fig. 5-8: The transmission data and R-matrix fits for the iron oxide samples enriched in ^{58}Fe, *vs.* neutron energy (below);

Resolution broadened total cross section for the pure isotope ^{58}Fe computed from the R-matrix resonance parameters (above).

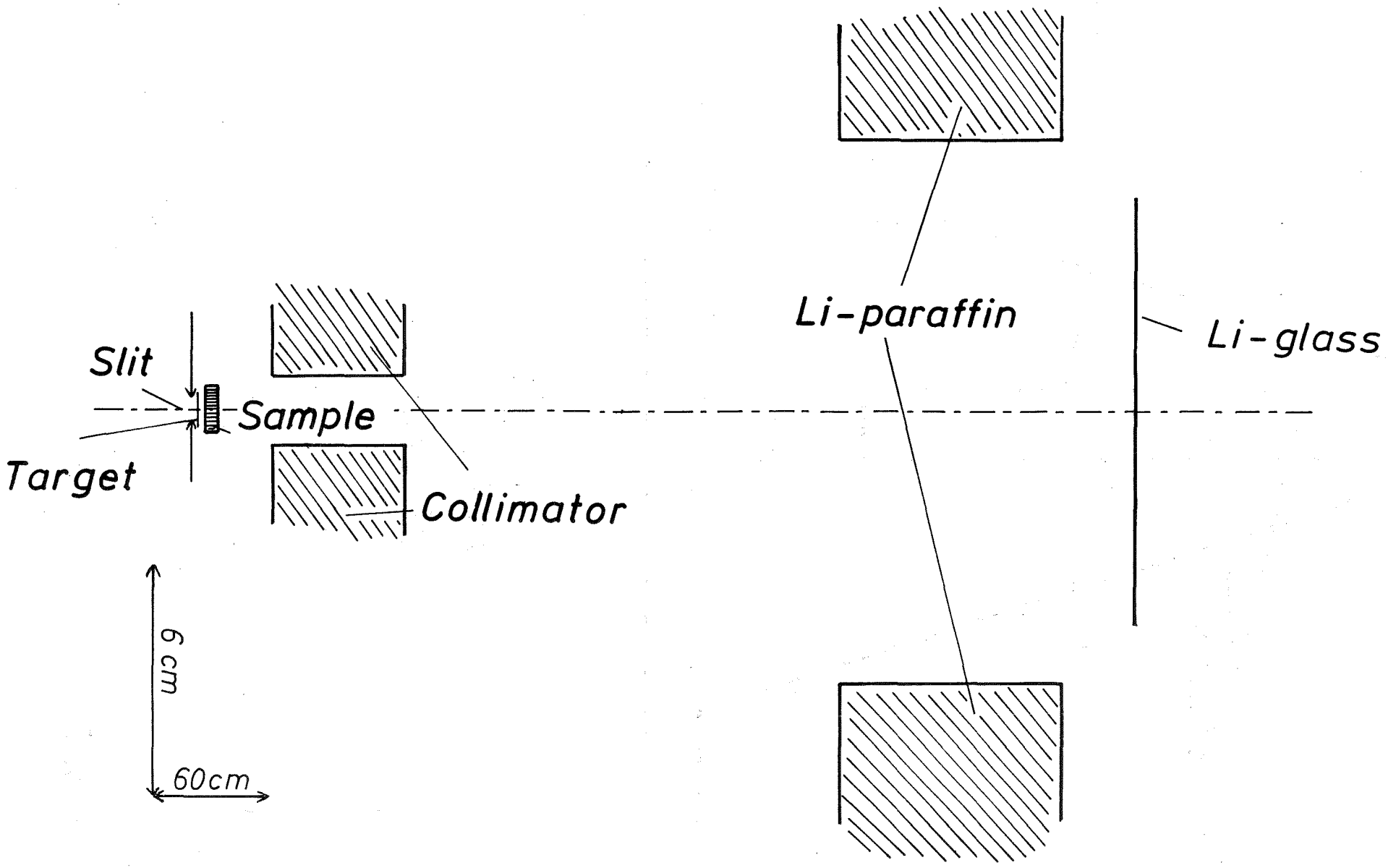
Slit
Sample
Target
Collimator
Li-paraffin
Li-glass
6 cm
60cm

Fig.1

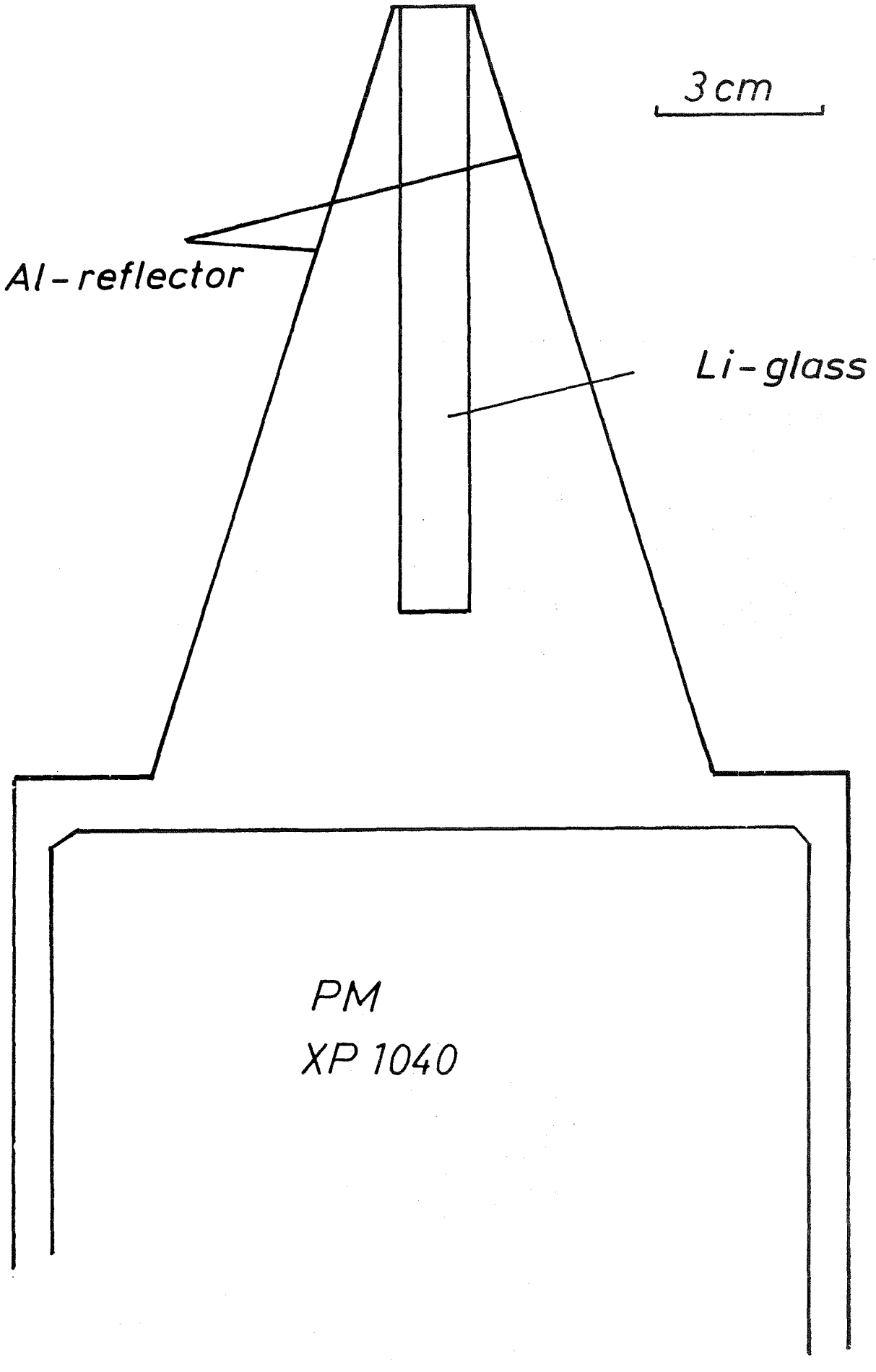

Fig. 2

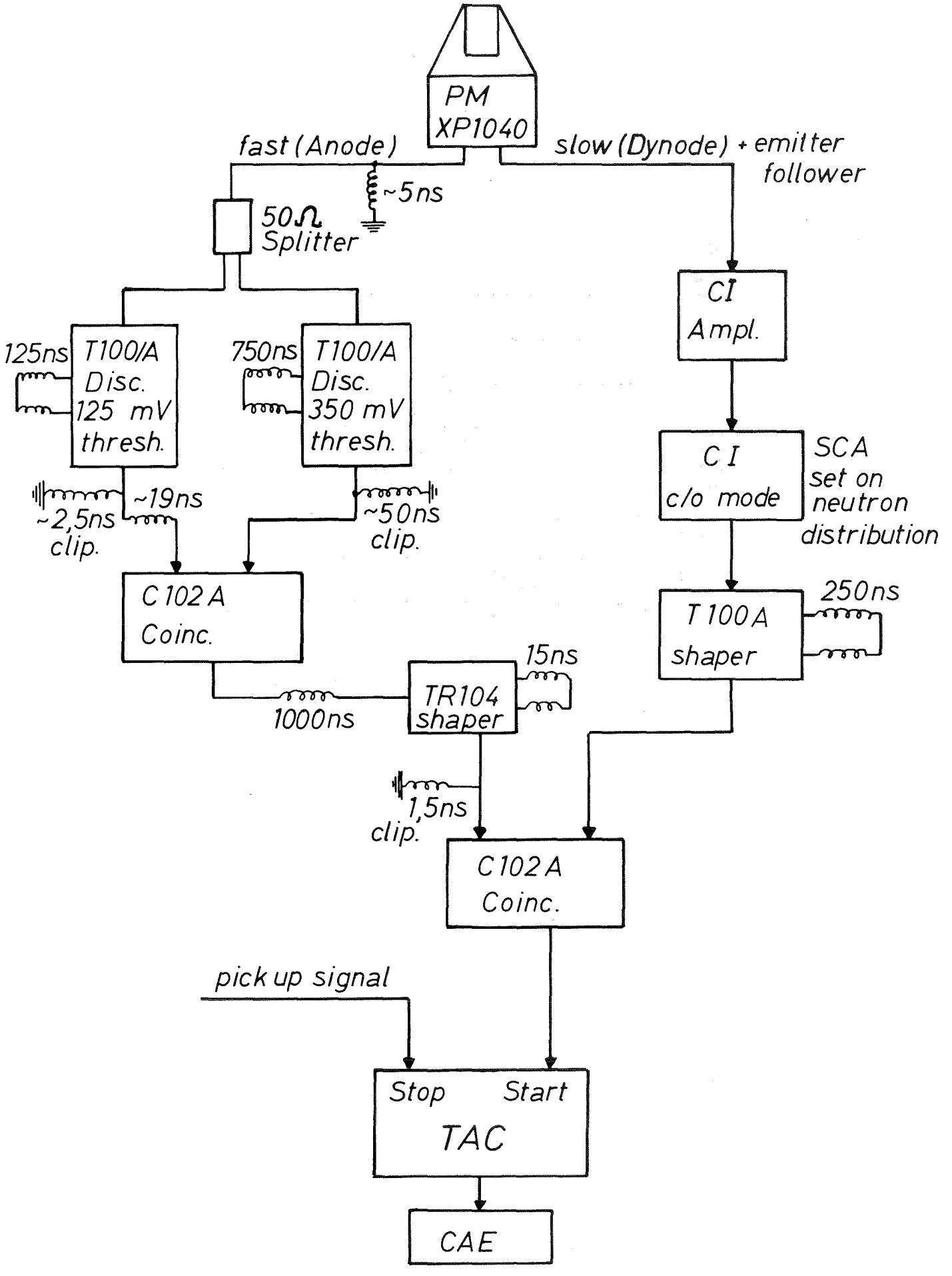
PM
XP1040
fast (Anode)
slow (Dynode) + emitter follower
~5ns
50Ω
Splitter
125ns
T100/A
Disc.
125 mV
thresh.
750ns
T100/A
Disc.
350 mV
thresh.
CI
Ampl.
~19ns
~2,5ns
clip.
~50ns
clip.
C I
c/o mode
SCA
set on
neutron
distribution
C102A
Coinc.
250ns
T100A
shaper
15ns
TR104
shaper
1000ns
1,5ns
clip.
C102A
Coinc.
pick up signal
Stop
Start
TAC
CAE

Fig.3

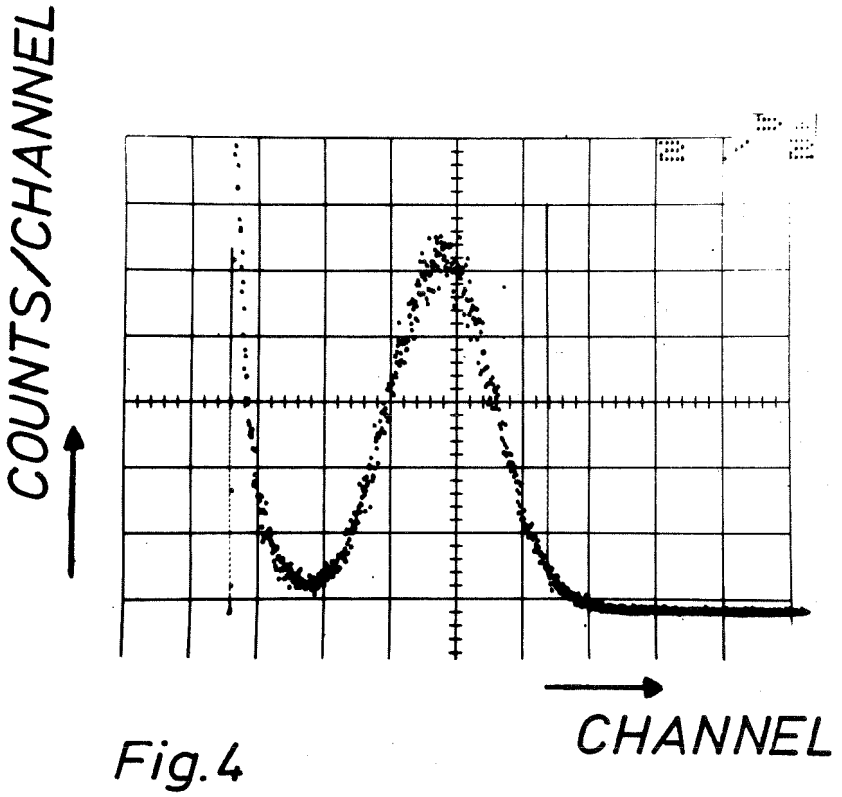

Fig. 4

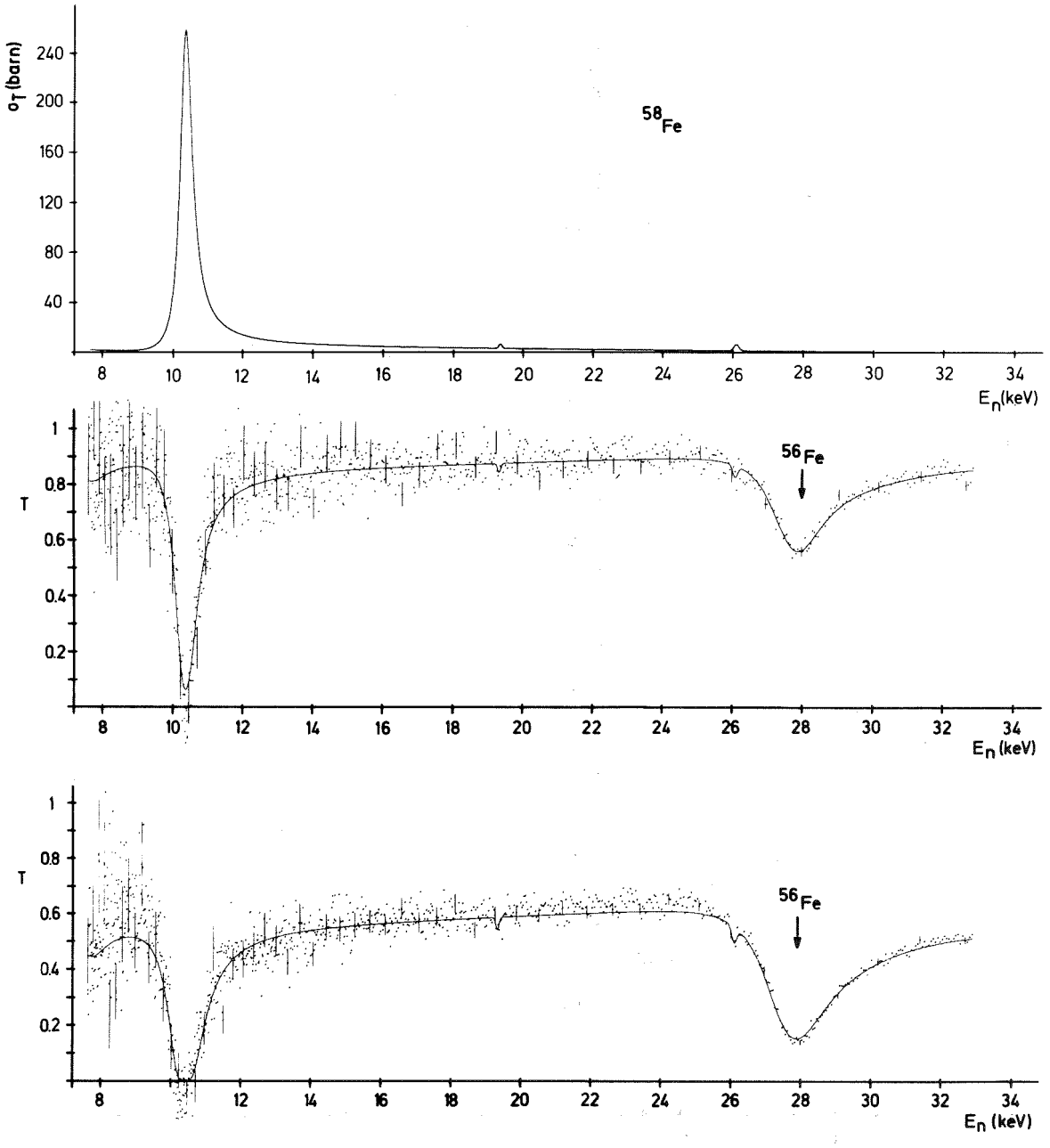
σ_T (barn)
240
200
160
120
80
40
^{58}Fe
8 10 12 14 16 18 20 22 24 26 28 30 32 34
E_n(keV)
T
1
0.8
0.6
0.4
0.2
^{56}Fe
8 10 12 14 16 18 20 22 24 26 28 30 32 34
E_n (keV)
T
1
0.8
0.6
0.4
0.2
^{56}Fe
8 12 14 16 18 20 22 24 26 28 30 32 34
E_n (keV)

Fig.5

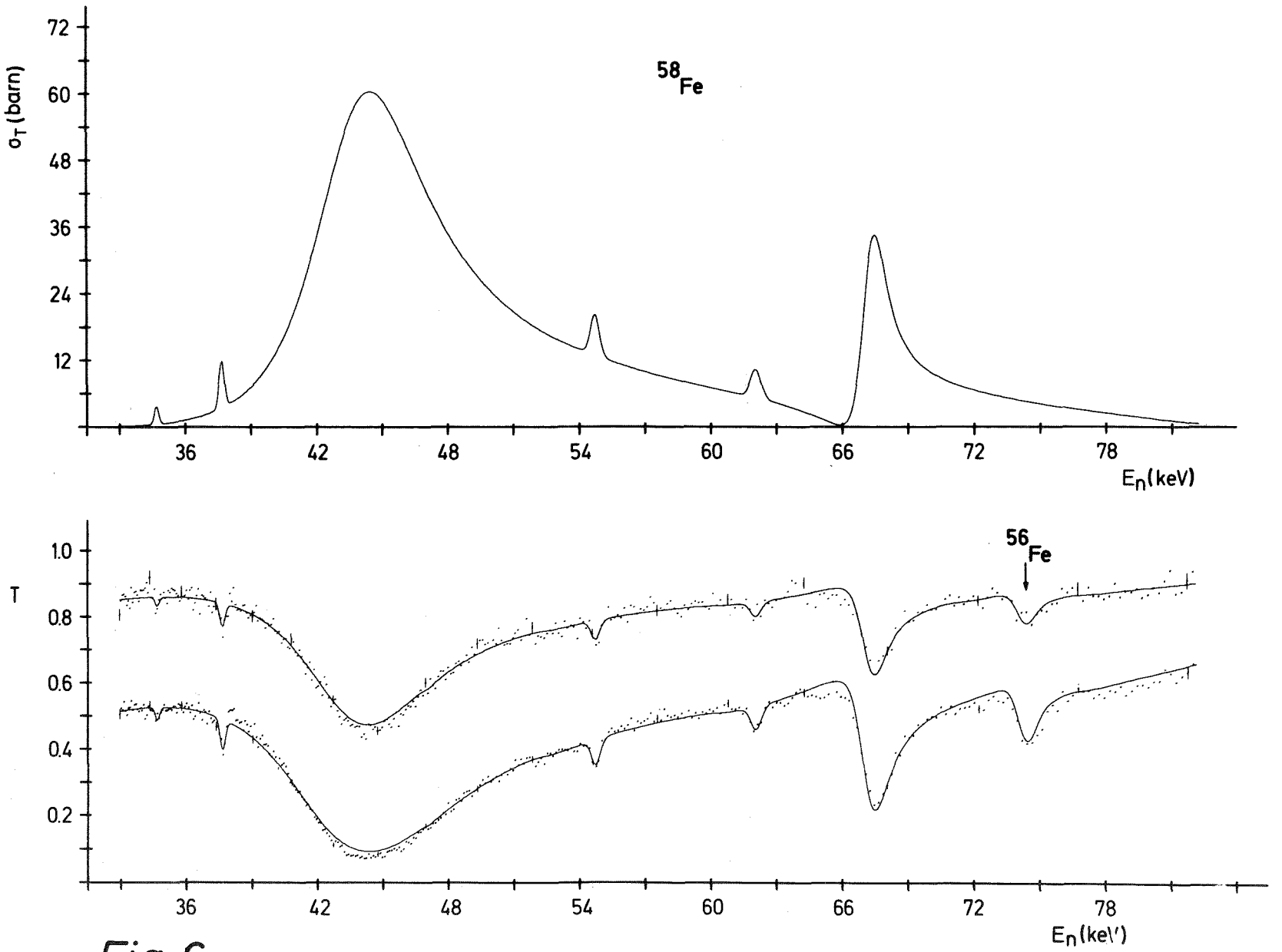
72
60
48
36
24
12
σ_T (barn)
^{58}Fe
36
42
48
54
60
66
72
78
E_n (keV)
1.0
0.8
0.6
0.4
0.2
T
^{56}Fe
36
42
48
54
60
66
72
78
E_n (keV)

Fig. 6

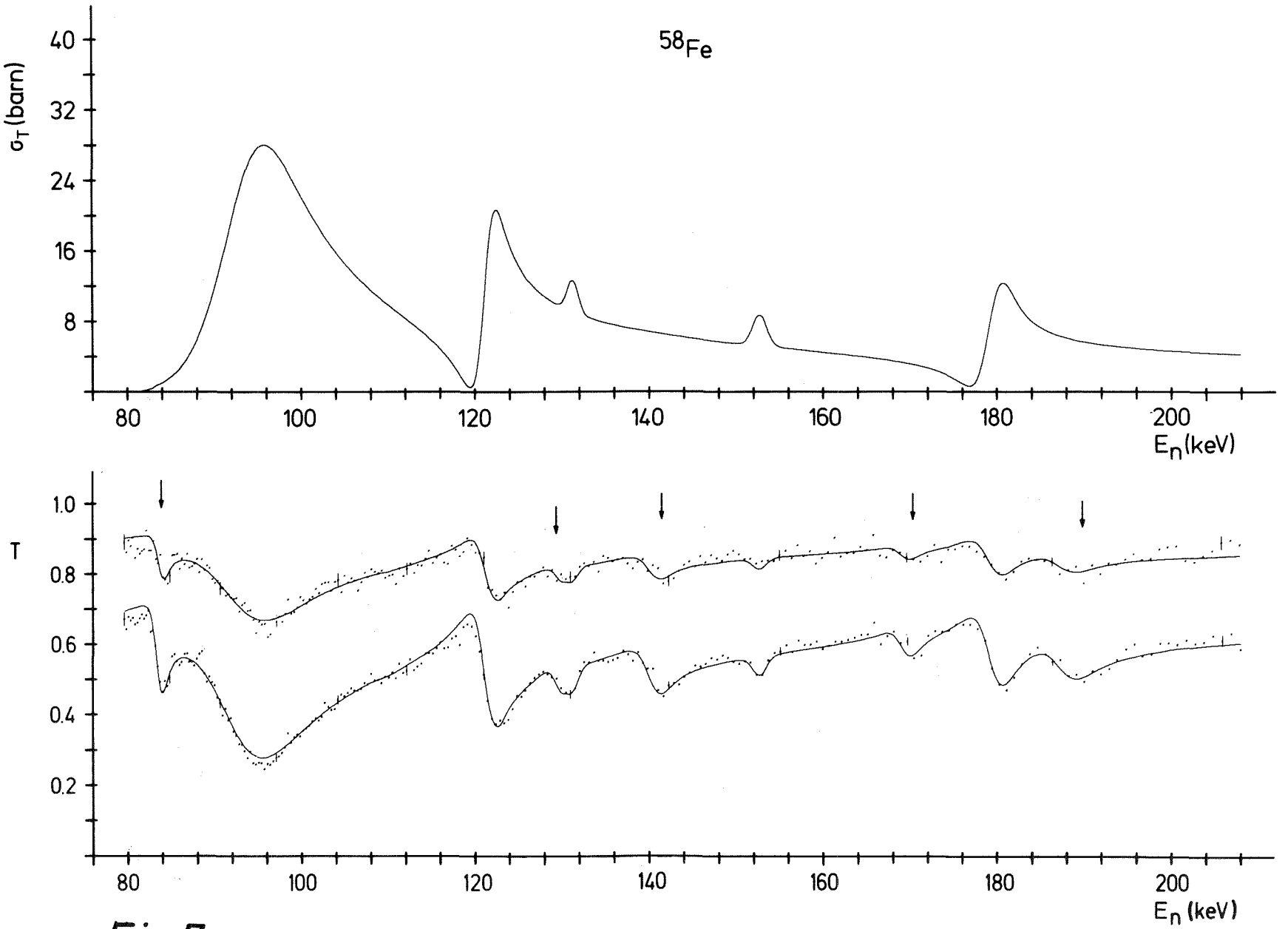
^{58}Fe
σ_T (barn)
40
32
24
16
8
80
100
120
140
160
180
200
E_n(keV)
T
1.0
0.8
0.6
0.4
0.2
80
100
120
140
160
180
200
E_n (keV)

Fig.7

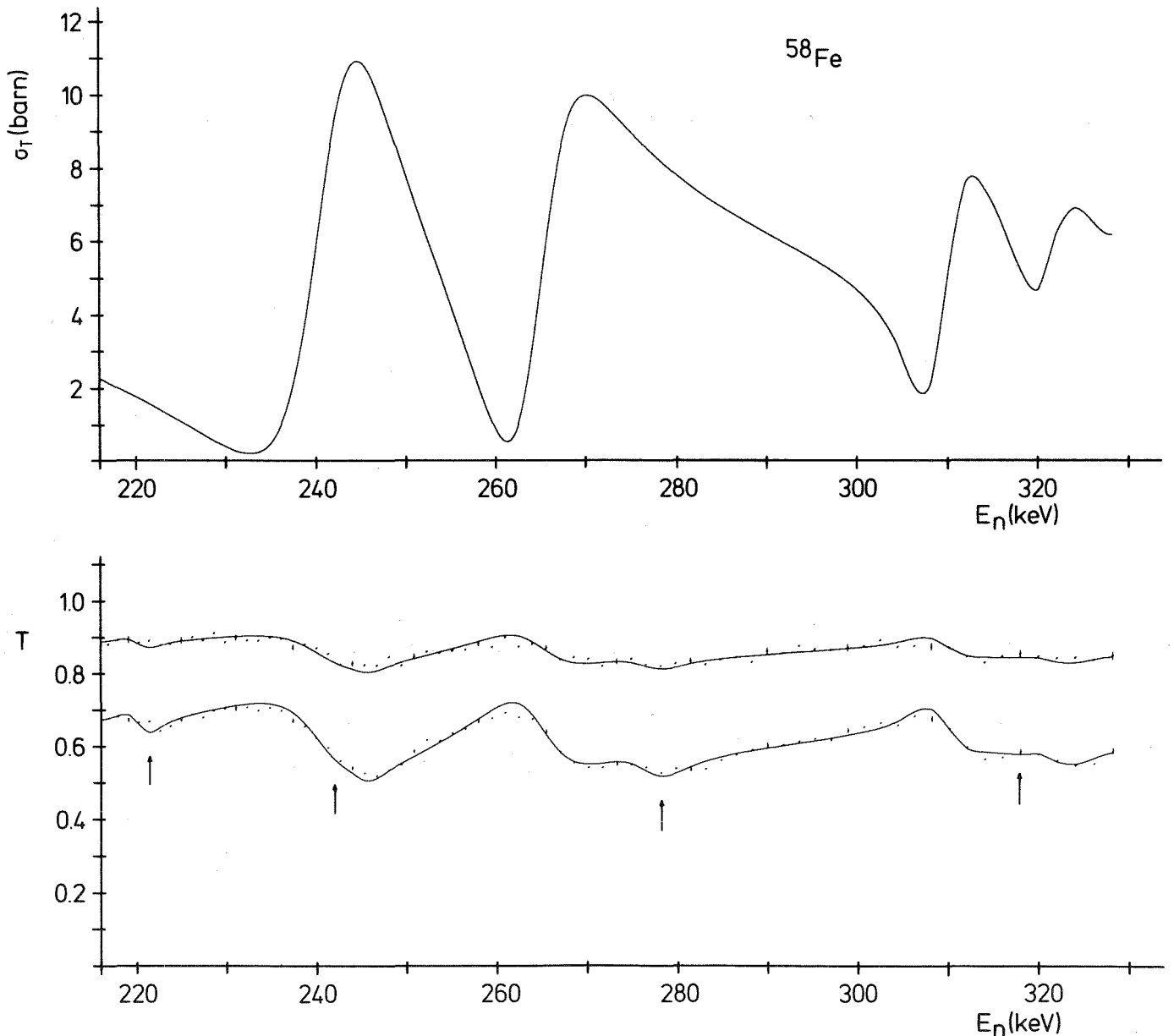
^{58}Fe
σ_T (barn)
12
10
8
6
4
2
220
240
260
280
300
320
E_n(keV)
T
1.0
0.8
0.6
0.4
0.2
220
240
260
280
300
320
E_n(keV)

Fig. 8